

JOUVENCE OF FLUOR: UPGRADES OF A FIBER BEAM COMBINER AT THE CHARA ARRAY

N. J. SCOTT^{*,§}, R. MILLAN-GABET^{†,¶}, E. LHOMÉ^{‡,||}, T. A. TEN BRUMMELAAR^{*,**},
V. COUDÉ DU FORESTO^{‡,††}, J. STURMANN^{*,‡‡} and L. STURMANN^{*,§§}

^{*}Georgia State University/The CHARA Array, Mount Wilson Observatory
Mount Wilson, CA 91023, USA

[†]California Institute of Technology, NASA Exoplanet Science Institute
Pasadena, CA 91125, USA

[‡]LESIA – CNRS, Observatoire de Paris, 92192 Meudon Cedex, France

[§]nic@chara-array.org

[¶]R.Millan-Gabet@caltech.edu

^{||}emilie.lhome@obspm.fr

^{**}theo@chara-array.org

^{††}vincent.forest@obspm.fr

^{‡‡}judit@chara-array.org

^{§§}sturm@chara-array.org

Received 2013 June 28; Revised 2013 September 9; Accepted 2013 September 9; Published 2014 January 6

The FLUOR (Fiber Linked Unit for Optical Recombination) interferometric beam combiner located at the CHARA Array on Mt. Wilson, California has recently undergone a program of major upgrades known as Jouvence of FLUOR (JouFLU). These upgrades seek to improve the precision, use, and observing efficiency of FLUOR as well as introduce new modes of operation. A Fourier Transform Spectrograph (FTS) mode and a spectral dispersion mode have been added to improve calibration and data collection. New mechanized stages and new cameras have been added to FLUOR for alignment and pupil plane imaging. Entirely new control/command software has been written for FLUOR which brings it into compliance with CHARA software standards. This allows for continued software upgrades and full remote operation capability. The new JouFLU instrument is now operating on sky and is expected to achieve accurate interferometric visibility amplitude measurements with 0.1 to 0.3% precision.

Keywords: Instrumentation: interferometers, techniques: high angular resolution, interferometric.

1. Introduction

Long baseline optical interferometry in astronomy is a unique and powerful technique with over a century of history. In the past decades it has emerged as a rapidly advancing field. Facilities such as the CHARA Array (ten Brummelaar *et al.*, 2005), NPOI (Armstrong *et al.*, 1998), SUSI (Davis *et al.*, 1999), and VLTI (Glindemann *et al.*, 2000) utilize this technology for astronomical investigations. Interferometry's ability to resolve the finest details possible from the ground enables astronomers to

study stars as more than points of light. Starspots, stellar atmospheres, debris disks, circumstellar environments, and compact binary systems among many other key points of interest may be studied in detail.

Pioneered by Albert Michelson, interferometry is in essence a technique of combining light while maintaining its phase. This results in what are called fringes or light and dark bands from constructive and destructive interference due to the wave nature of light. For astronomy, long baseline interferometry enables the use of multiple telescopes in order to achieve the resolving power of a much larger telescope. For an interferometer, the longer

^{††}Currently visiting scientist at the Center for Space and Habitability, Bern University.

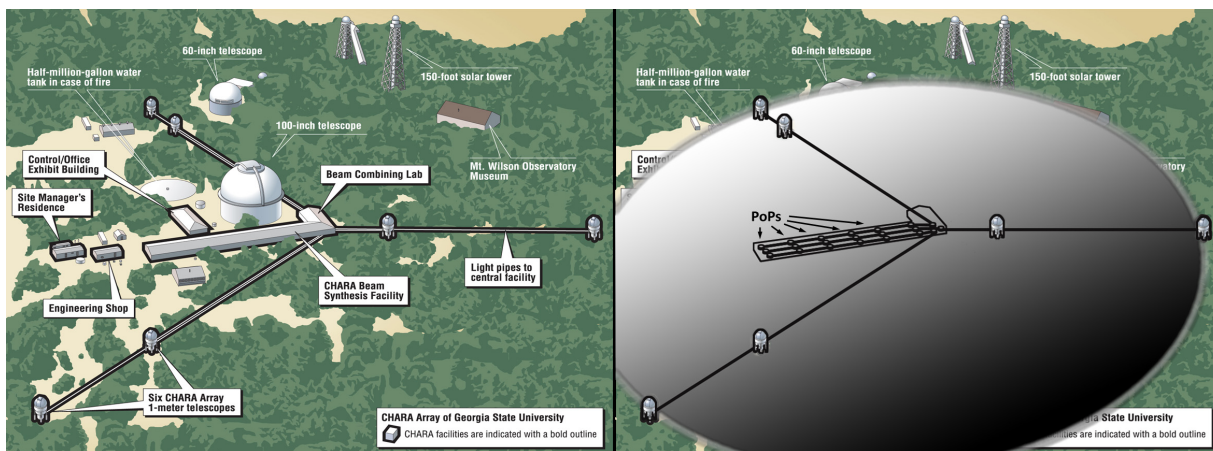


Fig. 1. Layout of the CHARA Array’s six telescopes, light pipes, and Beam Combining Lab within the context of the other facilities on Mt. Wilson (*left*). The illustration on the right shows the size of a mirror of equivalent resolving power to the CHARA Array. Also visible within the outline of the Beam Combining Lab are the “Pipes of Pan” (PoPs). Mirrors inserted at these points allow for various fixed intervals of large delay.

the baseline between telescopes the greater is its resolving power.

Georgia State University’s Center for High Angular Resolution Astronomy (CHARA) currently operates the longest baseline optical interferometer in the world at Mt. Wilson Observatory, California. This optical and infrared interferometer consists of six one-meter telescopes in a Y-configuration (see Fig. 1) and has baselines between 34 m and 331 m available. It has a maximum resolving power of $200 \mu\text{as}$ in the visible wave band. This would be equivalent to seeing details the size of a coin from 16,000 km away. The light from each telescope is conveyed via vacuum tubes to a central Beam Combining Facility. In this 100 m long building the individual light beams pass through a complex system of motorized carts and optics to ensure that each beam travels the exact same distance, in order to keep zero Optical Path Difference (OPD) throughout the night as the Earth rotates. Once the path lengths are equalized the beams are passed to a beam combining lab housing numerous instruments that perform scientific measurements of fringe visibility and phase. Full description of the CHARA Array is available in ten Brummelaar *et al.* (2005).

2. Instrument Overview

FLUOR (Fiber Linked Unit for Optical Recombination) is a high precision visibility instrument for interferometry. Built by the Laboratoire d’Etudes Spatiales et d’Instrumentation en Astrophysique

(LESIA) of the Observatoire de Paris, FLUOR produces some of the most precise measurements ever made in interferometry. Originally set up on Kitt Peak, Arizona in 1992, FLUOR was moved to the Infrared and Optical Telescope Array (IOTA) on Mt. Hopkins in 1995. FLUOR has been operating at the CHARA Array since 2002.

FLUOR is a two-way infrared interferometric beam combiner operating in the K' band ($\lambda = 2.20 \mu\text{m}$, $\Delta\lambda = 0.40 \text{ FWHM}$). It utilizes the spatial filtering properties of optical fibers to produce visibility measurements with a very high precision of $\approx 0.3\%$. See Coudé du Foresto *et al.* (1997) for a full discussion of the advantages of single-mode fibers in interferometry. For bright sources the statistical precision of FLUOR is only limited by the piston mode of atmospheric turbulence which introduces fringe jitter. Such precision allows FLUOR to make measurements of scientifically interesting features such as stellar radii that are accurate to the order of one percent or less.

The instrument is highly suited to the studies of debris disks (Absil *et al.*, 2006) and exozodiacal dust (di Folco *et al.*, 2007), young star circumstellar disks (Akeson *et al.*, 2005), Cepheid variable stars and Baade–Wesselink distance measures (Kervella *et al.*, 1999), binary star studies (Bruntt *et al.*, 2010), asteroeismology (Mazumdar *et al.*, 2009), and high dynamic range sources (Absil *et al.*, 2008). Such applications require observations at a dynamic range of 10^2 to 10^6 .

On the FLUOR bench, each of the two beams first encounter an OPD stage which has a payload

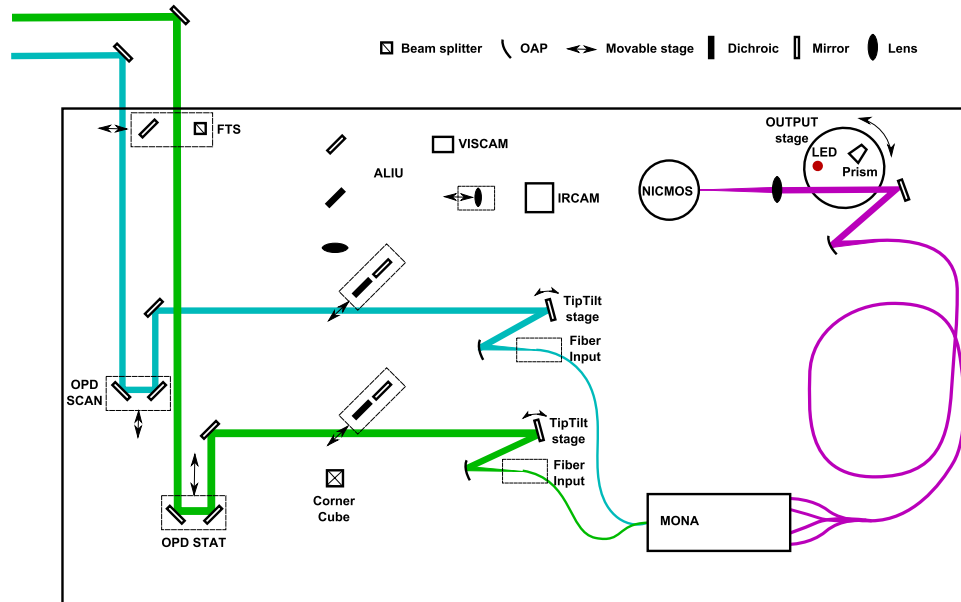


Fig. 2. JouFLU in the configuration used when observing. The alignment stages are out of the path of the beam and the OUTPUT stage is moved to the open position. Also shown for completeness are the optics of the alignment portion of the bench, see Fig. 7 for their use. The Fourier Transform Spectrograph beamsplitter is removed, see Fig. 5.

consisting of a set of two mirrors at 45° to the beam path (see Fig. 2). Following these stages each beam hits a fold mirror which directs the light to the motorized tip/tilt stages, which hold another fold mirror. These direct the light onto a gold coated $f/1.3$ 30° Off-Axis Parabola (OAP). The OAPs focus the light onto fiber injection stages capable of XYZ translation. The optical fibers are terminated in high precision E-2000 fiber connectors. These connectors allow the fibers to be unplugged and replugged without loss of alignment.

FLUOR interference fringes are produced by temporal OPD modulation using a mechanical stage which carries a mirror. The beam combination occurs within optical fiber couplers. The fiber couplers are located inside a closed box system called “MONA” built by Le Verre Fluoré. Two injection stages (Fiber input in Fig. 2) feed light into two Y-fiber couplers which in turn feed one of their outputs into a X-fiber coupler (see Fig. 3). Interferometric combination occurs in the X-fiber coupler. MONA outputs two photometric channels (PA and PB) from the Y-fiber couplers and two interferometric channels (I1 and I2) from the X-coupler. All four fibers join into a single fiber bundle in a $125\ \mu\text{m}$ square pattern. This bundle connects to another fiber translation stage and identical OAP. After the OAP the light enters an objective which images the fiber bundle onto the NICMOS science

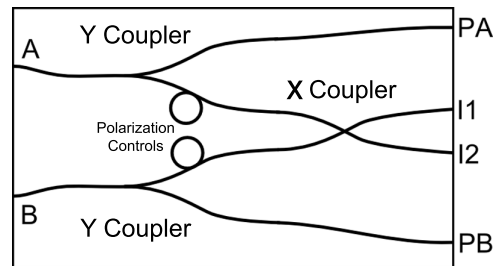


Fig. 3. The MONA fiber beam combiner consists of two Y-fiber couplers and one X-fiber coupler outputting one photometric channel for each beam and two interferometric channels total. Fiber polarization can be adjusted by changing the amount of bend to the fiber in the two loops.

camera which is read out as four pixels. The difference is taken between the two interferometric pixels to increase the Signal-to-Noise Ratio (SNR) while the photometric channels are recorded simultaneously for data calibration during the reduction stage (Coudé du Foresto *et al.*, 1997).

3. Upgrades to FLUOR

In recent years it became clear that several improvements could increase the efficiency, throughput, and integration of FLUOR with the CHARA Array. The Jouvence of FLUOR (JouFLU), loosely translated as “rejuvenation” of FLUOR, project has improved much of the optical bench setup of

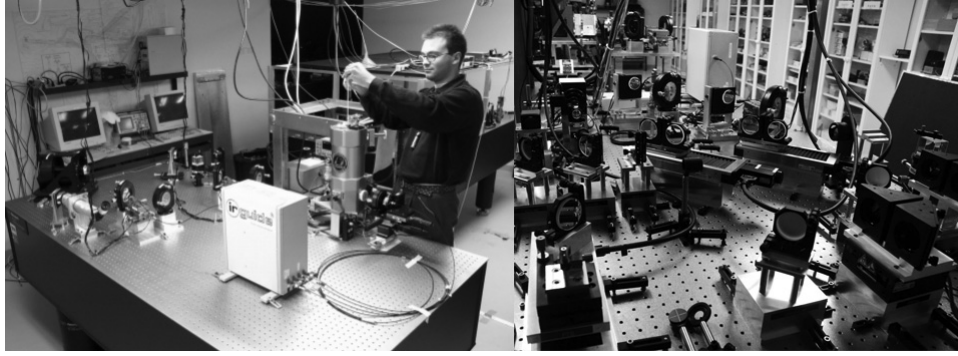


Fig. 4. FLUOR shortly after its move to the CHARA Array (*left*). JouFLU in its current condition in the CHARA lab (*right*).

FLUOR to provide greater opto-mechanical stability. This includes new motorized mounts for the mirrors that feed light into the optical fibers (Zaber model T-MM), new precision motorized stages which control the optical path length to generate fringes (OPD SCAN and OPD STAT), an infrared pupil plane camera system, a visible light alignment camera, and improvements to the science camera (NICMOS). Figure 4 shows the magnitude of the changes to the optical bench setup. In addition to the hardware upgrades a concurrent replacement of the control software system has produced an entirely new software system compliant with the CHARA operating environment, enabling JouFLU to be maintained at the cutting edge of improvements to other combiners at the array. As a combiner receives relevant new software features or tools, JouFLU may now benefit from them too with a minimum of effort. From these software changes FLUOR now has remote operation capability, potential for greater science data throughput, and higher statistical precision.

3.1. Optics

While most of the improvements from the JouFLU project center on new mechanical stages, several new optical elements were added as payload of these stages. Other optical elements were added to provide for new alignment techniques. The addition of a Fourier Transform Spectrograph (FTS) mode provides wavelength calibration of the science camera. In FTS mode a single beam is taken from CHARA. The single beam does not suffer from differential seeing and atmospheric piston. This allows longer scans at 100 Hz. The single beam is passed through a beamsplitter and fold mirror mounted on a motorized stage. The beamsplitter generates

the two beams necessary to feed into MONA for combination (see Fig. 5). OPD SCAN modulates the OPD. The resulting interferogram is affected only by the spectrum instead of spatial structure of the source. This spectrum can then be used to provide photometric and spectral calibrations of the instrument. This mode has not yet been tested.

The inclusion of a low dispersion ($R \approx 70$) biprism on the OUTPUT stage of JouFLU allows for the measurement of dispersed fringes across 7–11 channels. The simultaneous measurement of fringes will increase the statistical accuracy of the resulting measurement for sources bright enough to not be dominated by detector noise. The spectral dispersion mode will be of particular use when the science star and the calibrator star are of different spectral types. The measurement of visibilities in different wavelengths will enable the removal of chromatic bias/bandwidth smearing. Another use of the spectral dispersion mode is for the recording of differential phase. Normally with two beam interferometry no information of the phase is available. However, by measuring across multiple wavelengths the relative phase difference between wavelengths can be obtained. As a feasibility study of this technique spectrally dispersed fringes were recorded in 2004. The implementation of the spectral dispersion mode is planned for Fall 2013.

As part of the JouFLU project the fiber combiner box, MONA, was sent to Le Verre Fluoré for re-calibration and adjustment. The fiber heads were cleaned and two knobs with numbered scales were added to provide precise adjustment of the polarization of the fibers. Once installed back at the CHARA Array, interferometric signal throughput was maximized. This was achieved by scanning through the range of the polarization adjustment for each beam while measuring the visibility of lab

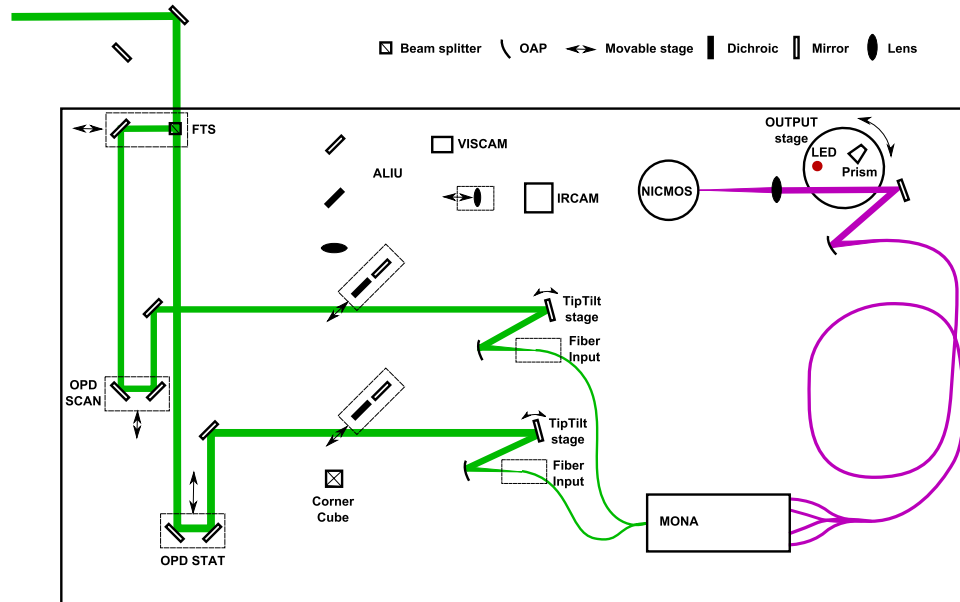


Fig. 5. FLUOR in the configuration used when calibrating with the Fourier Transform Spectrograph (FTS). The alignment stages are moved out, the FTS beamsplitter is moved into place, and OPD STAT changes position to compensate for the change in OPD.

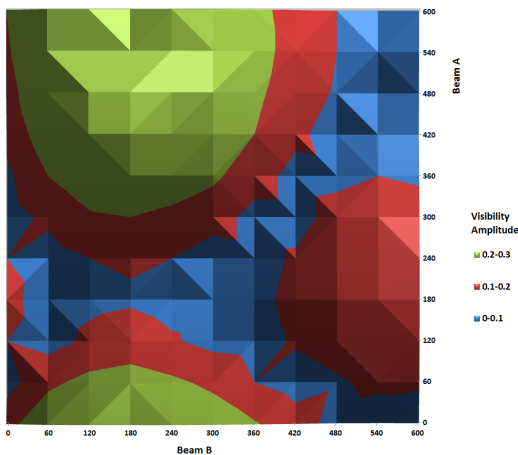


Fig. 6. The effects of adjustment of the fiber polarization for each of the two beams on white light fringe visibility. Each fiber has a knob which affects the bend of the fiber. Each knob was incrementally adjusted in steps of 60 arbitrary units to give 100 data points. Based on these results MONA was set to 480 and 180 for the top and bottom knobs, respectively.

fringes generated by a controlled white light source (see Fig. 6).

3.2. Mechanics

The most immediately apparent improvements to the FLUOR optical bench have been mechanical. Previously FLUOR consisted of fold mirrors, a

piezo-stack dither mirror to scan fringes, the OAPs to inject the fibers, and stepper motors to direct light to the OAPs. Alignments were done in the lab by hand and with an alignment telescope before the night's observations began. Now the addition of a Newport XPS Motion Controller/Driver has enabled the use of multiple mechanized stages to offer various configurations of the optical bench.

The Newport XPS Controller is capable of driving 8 axes of motion. We have connected 7 stages to the XPS. There is a stage for moving the FTS beamsplitter into position, two OPD stages, two alignment stages, a stage to adjust the focus for the H-band pupil camera, and the OUTPUT optics stage. The OPD and alignment stages are discussed in more detail below. The OUTPUT stage of JouFLU is a motorized rotating circular platform. It has three configurations: an open position for normal observations, a red LED for retro-injecting light for alignment procedures, and a ZnSe biprism to produce spectrally dispersed fringes.

The integrated interface and ethernet control of the XPS provides the ability to correct alignments or reconfigure the instrument while on sky without going into the lab, and opens the possibility for completely remote operations from any of the CHARA Remote Observing Control Rooms located in Atlanta, Meudon, Nice, Sydney, Ann Arbor, and Bonn.

3.3. Optical path delay

There are two Optical Path Difference (OPD) stages: OPD SCAN, a dynamic scanning stage which modulates the OPD and generates fringes within MONA, and OPD STAT, an adjustable static stage to correct residual OPD. These stages carry an identical payload consisting of a pair of mirrors. Movement of one of the OPD stages along the axis of the beam results in a change in the path length of twice the amount the stage moved.

The scanning stage meets rigid requirements as to linear velocity stability over its full range of travel. This stage was tested for such stability using laser metrology prior to installation and achieves $<1\%$ error in its velocity at $100\ \mu\text{m/s}$. In addition, further custom tuning was performed by a Newport technician. The stage is powered by a linear DC motor and has 50 mm of travel. The greater range of travel for this new stage greatly surpasses the $200\ \mu\text{m}$ of the FLUOR piezoelectric dither mirror. The increased range is necessary for the use of FTS mode. During normal observation mode and collecting fringes at 100 Hz the scanning stage travels at $105\ \mu\text{m/s}$ (half the optical path velocity due to double pass) over a range of $150\ \mu\text{m}$. For FTS mode the stage travel range must be 10 times this. The exact velocity of the OPD SCAN stage is determined by the NICMOS camera readout frequency. Fringes are temporally modulated and scanned at a rate of 5 samples per fringe (2.5 times Nyquist). So for 100 Hz fringes NICMOS reads out at 500 Hz (2 ms). The XPS Motion Controller has been programmed to send a signal to the JouFLU control computer to report when the OPD SCAN stage is moving at a constant velocity. The JouFLU computer then only requests data from NICMOS when this is true. This ensures that the fringes are only recorded under the constant velocity situations and not when the stage is accelerating.

The second stage, OPD STAT, does not have the strict velocity requirements of OPD SCAN; however it needs longer travel. This stage corrects for the offset created by the introduction of FTS beam splitter. Approximately 4 centimeters of path difference are introduced in FTS mode due to the separation of the two beam paths (see Fig. 5).

3.4. Alignment

A major focus of JouFLU is to improve the quality and ease of optical alignment procedures

to increase the observing efficiency of FLUOR. The addition of ALIignment Units (ALIU) improves the accuracy and repeatability of alignment for the beams. These new stages also add the ability to view both the image and pupil planes. Previously FLUOR alignment procedures could only be performed during the day before observations and required personnel to be in the lab. The addition of ALIU provides a method for reliable alignment adjustments to be performed during the night with little interruption of data collection, or to be performed remotely. ALIU consists of two long travel Newport stages, one for each beam, which carry a payload of a mirror and a dichroic. These stages are placed at 45° to the beam path and have three set positions: Open, Dichroic, and Mirror. During science observing ALIU is clear of the beam path. When an alignment needs to be performed one of the stages can position the dichroic into the path of the beam that is to be aligned (see Fig. 7). Then on the JouFLU OUTPUT stage a red LED is turned on and rotated into position to be retro-injected through MONA. After leaving the fibers the light from the LED hits the ALIU dichroic and is reflected to a corner cube. The corner cube directs the light to pass through the dichroic and to another system consisting of a mirror and focusing lenses (see Fig. 8). The LED spot is imaged by a Prosilica visible light camera. The position of this spot is compared with that of a green laser spot produced by CHARA. The motorized tip/tilt stages are then adjusted to overlay the two spots and conjugate the system. The final possibility is the insertion of a mirror which directs light to the InGaAs detector, which allows the pupil plane to be viewed. This pupil camera operates in the H band and allows problems such as vignetting and other issues leading to a loss of flux to be diagnosed during on-sky operations.

Viewing the CHARA pupil is accomplished with a new camera that operates in H-band ($0.9\text{--}1.7\ \mu\text{m}$) and is situated next to the visible alignment camera. This camera is a commercially available electronically cooled 320×256 InGaAs detector. The use of $1.319\ \mu\text{m}$ metrology laser by the array necessitated the inclusion of two notch filters to prevent possible damage to the pupil plane camera. To utilize the pupil camera either of the ALIU stages move to the mirror position. The beam passes through a lens and is then redirected at a right angle with a dichroic. It passes through the two notch

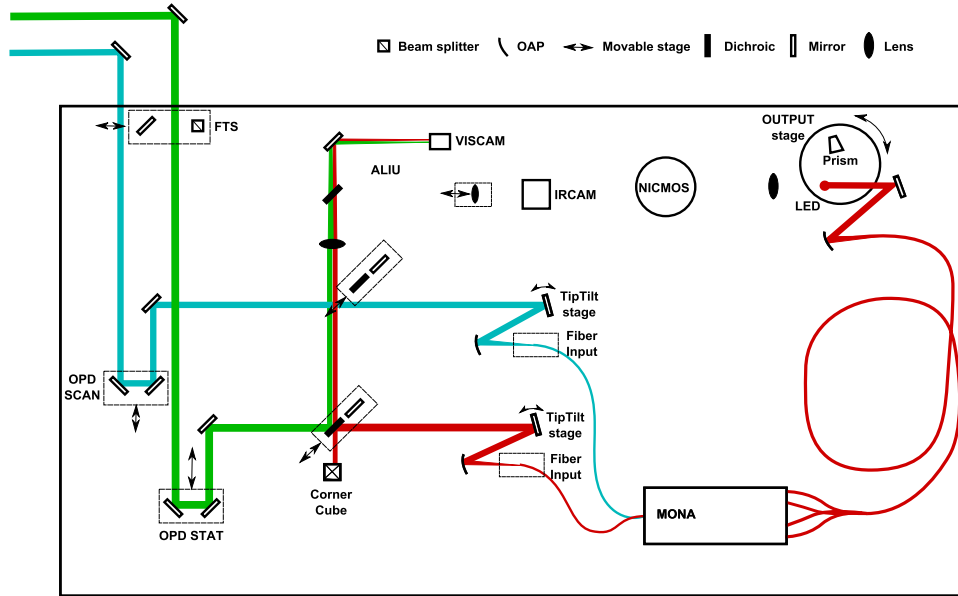


Fig. 7. JouFLUOR in the configuration used when aligning the fiber injection. One of the alignment stages is moved to the dichroic position and the output stage is moved to the LED position. The LED projects red light back through MONA and to the ALIU dichroic. The tip/tilt stage is adjusted to center the JouFLUOR LED source with the CHARA white light source. The alignment stage is then moved out and the process can be repeated with the other beam. Figure 8 shows more detail of this section of the bench.

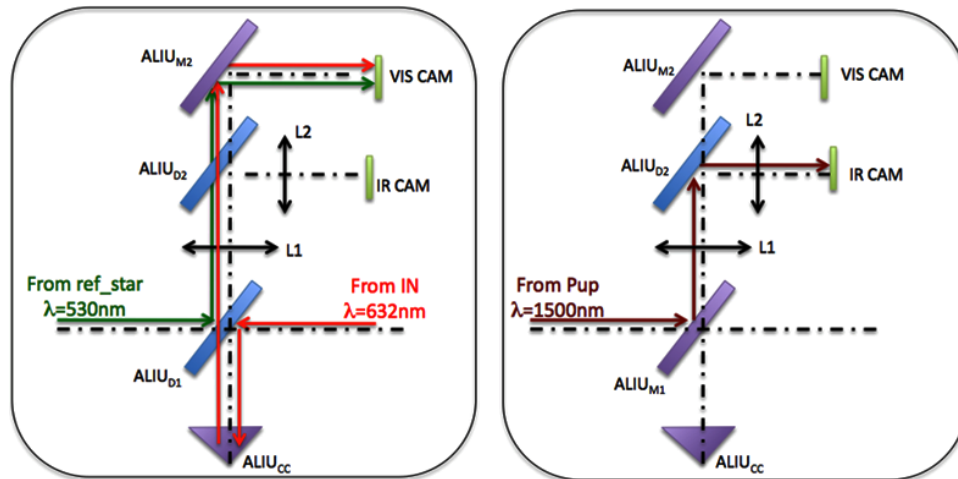


Fig. 8. FLUOR in the configuration used when aligning with the ALIU system and the visible camera (VISCAM). The ALIU stage for the desired beam is moved to the dichroic position and the light from the external source or star passes through a focusing lens (L1) and another dichroic (D2) to reach a fold mirror (M2) which directs it to the alignment camera (*left*). To check the CHARA pupil for vignetting or other possible loss of flux an ALIU stage is moved to the mirror position and an external source light is passed through the same lens used by the VISCAM, reflects off of dichroic D2, and reaches a focusing lens mounted on a stage (L2). The CHARA pupil is then recorded with the infrared camera (*right*). (Image credit: LESIA – CNRS/Observatoire de Paris.)

filters and a focusing lens. The global response function for this system is shown in Fig. 9.

To take full advantage of this new alignment capability a greatly improved fiber injection system has been added to JouFLUOR. The previous mirror mounts which directed light onto the OAPs and into

the optical fibers were actuated by stepper motors. These stepper motors were not precise enough to produce repeatable alignment for fiber injection. These mirror mounts have been replaced by Zaber tip/tilt stages. The minimum step size of these stages is 310 mas or 1/20 of the 6.5 μm core diameter

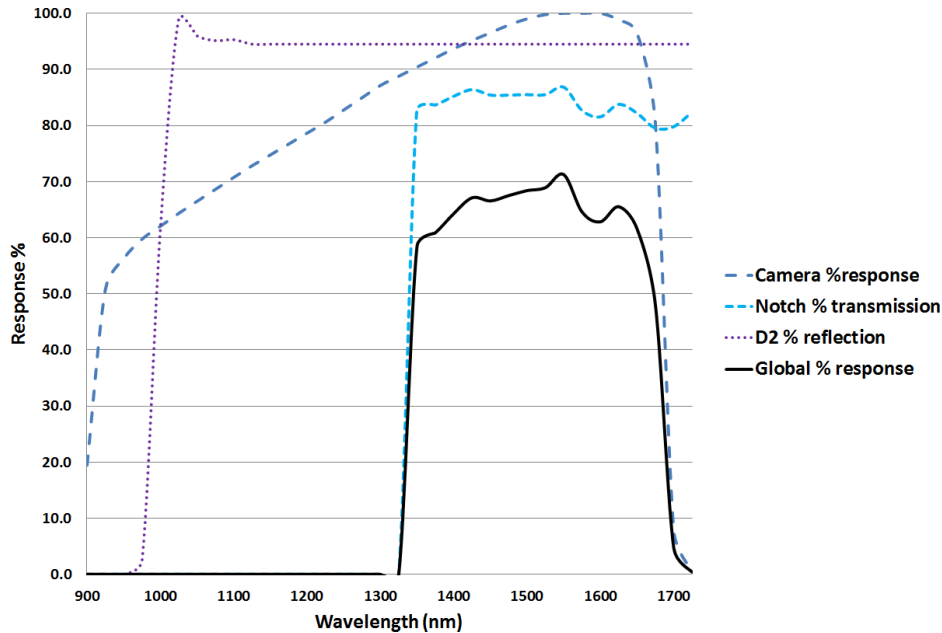


Fig. 9. The global response function for the H-band pupil imaging camera. Also plotted are the response functions for a single notch filter, the camera response function, and the dichroic (D2) reflection function. The global function is the product of the camera’s response, the two notch filters, and the D2 reflection.

of the fibers. In practice a step size of $\approx 1.2 \mu\text{m}$ is used to improve repeatability of raster scans. This is a large improvement over the previous stepper motors which had a step size roughly equal to the fiber core diameter. The higher precision injection of light allows for accurate raster scanning to maximize the amount of light that reaches MONA. The Zaber tip/tilt stages are also much faster than the previous stepper motors which allows for faster and larger raster scans. Software has been written to allow multiple default positions for these stages to be set depending on the configuration of the instrument.

3.5. Software

The previous Command/Control system for FLUOR consisted of software originally written for use while FLUOR was at IOTA. The software was written in LabView and operated parallel to the normal functions of CHARA. As such it was unable to take advantage of some of the features present at the CHARA Array due to the integrated software environment. To remedy this the FLUOR software system was rewritten as the JouFLU server and GUI. This required an extensive ground-up conversion of the LabView code to C code modeled on existing CHARA beam combiner functions. There are several major advantages to the

new software system. Operation from any CHARA remote facility are now possible. JouFLU will be kept up to date with any system software updates to the CHARA operating environment. JouFLU data can be reduced using a modified version of the very well understood “Classic” CHARA data reduction code. With the new software JouFLU can be integrated with other CHARA systems such as the fringe tracker, CHAMP (CHARA-Michigan Phase tracker).

3.6. Camera

The four outputs (2 interferometric, 2 photometric) of the MONA combiner are imaged onto four pixels of a NICMOS3 array, housed in a camera originally developed for the IOTA interferometer Millan-Gabet *et al.* (1999). We use the same dewar, readout electronics and control software approach as in the original implementation. In 2007 however, the original NICMOS3 array failed, and was replaced by another engineering grade NICMOS3 array, kindly loaned by NOAO. Although the replacement array has a larger number of bad pixels, which can easily be avoided, the noise characteristics remain similar. Camera control has been integrated into the CHARA environment as described in Sec. 3.5. The main JouFLU CPU coordinates the Newport XPS and the MS-DOS machine that communicates

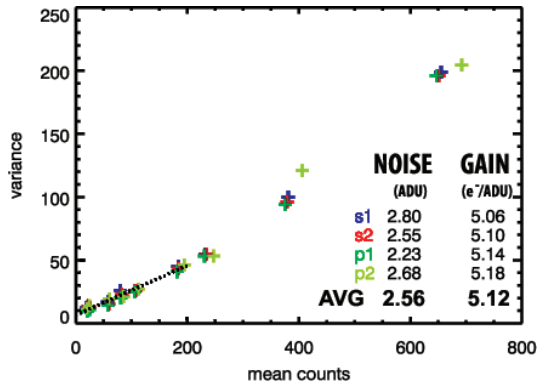


Fig. 10. The results of gain and readout noise tests of the NICMOS camera for each of the four read pixels. The camera was operated in destructive mode at 500 Hz with 2 loops and 3 reads of each pixel. Measurements were determined by calculating mean counts and variance as light levels were incrementally increased. The first 200 counts were treated as linear and a regression was performed to determine the gain. Mean readout noise for the four pixels read is 2.56 ADU with a mean gain of 5.12 e⁻/ADU.

with NICMOS. The Newport XPS directly triggers reading of the camera so that data is only collected when the fringe scanning stage (OPD SCAN) is moving with constant velocity. These data are then sent to the JouFLU computer for real time display and recording.

In Fig. 10 we show the results of updated measurements of the camera gain and readout noise, performed using the standard method of measuring the flux-variance curve, and using the same readout

mode as is used for on-sky observations of the four target pixels. As in previous implementations, we use Fowler sampling for noise reduction: the array is reset for each sample, after which the pixels of interest are sampled continuously as they discharge Fowler & Gatley (1991). The integration time for each recorded data point is set by the time needed to sample each target pixel, possibly multiple times. For a given camera read frequency an optimum number of reads and loops for the pixels is determined to give the correct sample time and minimize read noise. For example to get a 500 Hz camera readout the four pixels are read out 11 times in one loop. This combination was found to give a 2 ms readout with minimal readout noise. The timing of pixel readout for various modes was checked by oscilloscope. Figure 11 shows noise reduction as a function of the number of multiple reads per sample (i.e., per data point in the fringe scan).

To date the faintest unresolved star observed with JouFLU is HD102647, which has $K_{\text{mag}} = 1.9$. Using the fringe contrast (visibility) SNR in these data, we estimate a point-source limiting magnitude for JouFLU of $K = 6$. This compares well with expectations based on the above measurements of camera noise and on modeling the optical efficiency through CHARA and JouFLU. As JouFLU now moves from the engineering phase to actively collecting science data we expect to refine this limit as data is collected on fainter targets.

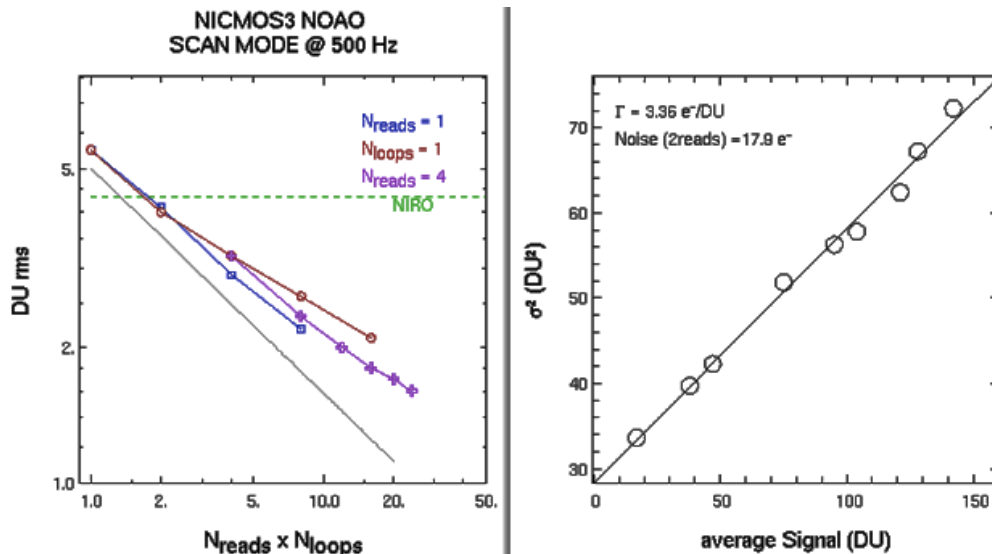


Fig. 11. Early tests of the NICMOS camera showing effect of changing the number of times a pixel is read/looped (Left) and the gain and readout noise under increasing amounts of flux (Right). Figures from Antoine Mérand, March 2007.

4. Status

JouFLU has obtained fringes on the sky as of May 2012 and is on line for regular operation during 2013. Preliminary observations have already begun and several FLUOR runs are scheduled for this observing season. A complete realignment of the JouFLU bench has been completed as well as development of new alignment procedures. Tests are underway to determine the limiting sensitivity and science throughput of the instrument.

5. Future

Looking ahead there are plans to implement further upgrades to add capability to JouFLU. As already mentioned in Sec. 3.1 there are plans to implement a mode to collect spectrally dispersed fringes and Fourier Spectrograph mode. NICMOS currently operates through a PC serial connection; it will be upgraded to ethernet readout. This should greatly improve the communication speed of the camera. Improvements planned for the software include general updates for usability, more tests of remote operation, and the addition of new modes of observation such as FTS and spectral dispersion. Refinements to the camera readout software will add more flexibility to reading the camera as well as on-the-fly changes of the Regions of Interest (RoIs).

Future improvements will include modification to work with a newly available feature of the CHARA Array, a fringe tracker called CHAMP Berger *et al.* (2008). CHAMP should enable much higher precision data to be obtained with JouFLU by reducing or removing the remaining atmospheric piston error. This will allow longer tracking of fringes and a higher quantity of shorter scans, increasing the data throughput and statistical precision. This should lead to higher accuracy measurements of raw visibility. Fringe tracking will also improve observation during periods of high atmospheric turbulence. This will increase the observing efficiency of the instrument.

The CHARA Array has begun work on bringing adaptive optics to the six telescopes of the interferometer. FLUOR will be among the five other beam combiners at the CHARA Array to benefit from this.

6. Conclusions

FLUOR was a productive high precision instrument that fulfilled a niche for high precision visibility

measurements at the CHARA Array. The new upgrades that have been introduced continue that role while adding much needed improvements. JouFLU adds higher efficiency, increased data throughput, new capabilities, greater ease of use, and more accessibility to this established instrument. The addition of a Fourier Transform Spectrograph mode and the option of collecting spectrally dispersed fringes offers new possibilities for science with JouFLU. The integration with the CHARA Array allows remote operation as well as rolling updates to the software control systems and data reduction software. The prospect of better alignment leading to higher throughput and faster data collection from improved stages should allow higher precision visibilities.

JouFLU will have a significant impact on the performance of FLUOR. While quantitative estimates of improvements at the system level are always speculative without full end-to-end modeling of the instrument, our goal is to realize a threefold gain in precision and accuracy reaching 0.1% calibrated visibility amplitude measurement for a single observation bracket. Once all aspects of the upgrade and the new data reduction pipeline have been optimized we expect a gain of one magnitude in sensitivity, pushing the magnitude limit to $K = 6$ or fainter. Our confidence comes from early results which have shown improvements in achieving fringes both in the laboratory and on the sky.

Acknowledgments

The CHARA Array, operated by Georgia State University, was built with funding provided by the National Science Foundation, Georgia State University, the W. M. Keck Foundation, and the David and Lucile Packard Foundation. The CHARA Array is currently funded by the National Science Foundation under Grant AST-0606958. Additional funding for the Jouvence of FLUOR upgrade project was provided by ANR EXOZODI. Research conducted with FLUOR has made use of NASA's Astrophysics Data System and of the SIMBAD database, operated at CDS (Strasbourg, France).

References

- Absil, O., di Folco, E., Mérand, A. *et al.*, 2006, *A&A*, **452**, 237.
- Absil, O., Defrère, D., Coudé du Foresto, V. *et al.*, 2008, *Proc. of SPIE*, 7013.

- Akeson, R. L., Walker, C. H., Wood, K. *et al.*, 2005, *ApJ*, **622**, 44.
- Armstrong, J. T., Mozurkewich, D., Rickard, L. J. *et al.*, 1998, *ApJ*, **496**, 550.
- Berger, D. H., Monnier, J. D., Millan-Gabet, R. *et al.*, 2008, *Proc. of SPIE*, 7013.
- ten Brummelaar, T. A., McAlister, H. A., Ridgway, S. T. *et al.*, 2005, *ApJ*, **628**, 453.
- Bruntt, H., Kervella, P., Mérand, A. *et al.*, 2010, *A&A*, **512**, A55.
- Coudé du Foresto, V., Ridgway, S. & Mariotti, J.-M., 1997, *A&APS*, **121**, 379.
- Coudé du Foresto, V., Perrin, G., Ruilier, C. *et al.*, 1998, *Proc. of SPIE*, **3350**, 856.
- Coudé du Foresto, V., Borde, P. J., Merand, A. *et al.*, 2003, *Proc. of SPIE*, **4838**, 280.
- Davis, J., Tango, W. J., Booth, A. J. *et al.*, 1999, *MNRAS*, **303**, 773.
- di Folco, E., Absil, O., Augereau, J.-C. *et al.*, 2007, *A&A*, **475**, 243.
- Fowler, A. M. & Gatley, I., 1991, *Proc. of SPIE*, **1541**, 127.
- Glindemann, A., Abuter, R., Carbognani, F. *et al.*, 2000, *Proc. of SPIE*, **4006**, 2.
- Kervella, P., Coudé du Foresto, V., Traub, W. A. & Lacasse, M. G., 1999, Working on the Fringe: Optical and IR Interferometry from Ground and Space, **194**, 22.
- Lhomé, E., Scott, N., ten Brummelaar, T. *et al.*, 2012, *Proc. of SPIE*, **8445**.
- Mazumdar, A., Mérand, A., Demarque, P. *et al.*, 2009, *A&A*, **503**, 521.
- Millan-Gabet, R., Schloerb, F. P., Traub, W. A. & Carleton, N. P., 1999, *PASP*, **111**, 238.
- Perrin, G., 2003, *A&A*, **398**, 385.